ChemSusChem

Research Article
doi.org/10.1002/cssc.202301786

Chemistry Europe
European Chemical Societies Publishing

www.chemsuschem.org

Lignosulfonate-Based Carbon-Supported Pellets Catalyst to Enhance Sustainable Biofuel Production from Waste Cooking Oil

Ingrid F. Silva,*[a] Irina Shekova,[a] Antje Volkel,[a] Majd Al-Naji,[b] and Markus Antonietti*[a]

In this study, a cost-effective and stable heterogeneous acidic carbocatalyst (CZnLS950) derived from Na-lignosulfonate (LS), a side product of the paper industry, was employed to produce hydrocarbon fuels through the pyrolysis of waste cooking oil (WCO) and crude natural-oil extracted from sunflower seeds, aligning with the principles of the circular economy. To enhance its practicality in industrial settings, the catalyst was synthesized in pellet form, enabling easy separation from the biofuel produced during the reaction. CZnLS950 exhibited remarkable catalytic efficiency in the pyrolysis of WCO, resulting in a 71 wt.% liquid biofuel yield under mild conditions. This performance is attributed to the unique synthesis procedure of acidic carbocatalyst, which utilizes LS and nano ZnO (20 nm) to create a hierarchical pore structure with acidic properties (1.1 mmol of NH_3 g^{-1}). Stability and reusability of the carbocatalyst were evaluated, and the results showed excellent stability with small catalytic deactivation (~5 wt.%) after the fourth use. Attempts at distinct catalytic mechanisms for WCO and sunflower seeds crude natural-oil pyrolysis were provided to understand the processes involved in obtaining the two different biofuels produced. Overall, this study sets the stage for exploring Lignosulfonate-based materials to achieve renewable biofuel from recycling streams.

Introduction

Rapid economic and social development combined with population growth in recent years have led to higher energy demands and accelerated depletion of fossil fuels.[1] In order to obtain alternative fuel sources, the production of renewable energy has been expanding worldwide driven by increasing fossil fuel prices, engagements to greenhouse gas reductions and government incentives. For example, the EU has a target of achieving climate neutrality by 2050 stipulated by the International Energy Agency's Net Zero roadmap.[2] Moreover, the EU parliament has raised the bar for greenhouse gas reductions by 2030 from 30% to 40% compared to 2005 levels.[2] As part of the Paris Agreement in 2015, many other countries, such as Brazil and the United States committed to reducing their emission of 50% by 2030, compared to 2005 emissions, aiming to reach carbon neutrality by 2050.[3,4]

In this sense, biofuel production is a nearby sustainable alternative to replace non-renewable liquid fossil fuel-derived.[5,6] Biofuels can be produced through different processes, including transesterification, esterification and thermal cracking or pyrolysis of fats and plant oils.[1,5] Among all these methods, combining fast pyrolysis of waste cooking oil (WCO) with catalysts to reduce oxygen content and increase hydrocarbon yield to produce high-quality hydrocarbon fuels has great potential to be an alternative energy source.[7] The use of WCO diminishes biofuel synthesis costs and environmental pollution, besides contributing to the circular economy.[8,9] For example, a current practice using waste-derived feedstocks for the generation of sustainable aviation fuels (SAF) is strongly encouraged in the EU, underscoring the growing demand for robust processes capable of utilizing low-quality and low-cost feedstock.[10] In addition, global vegetable oil consumption has increased from 150 million metric tons (MMT) in 2013/14 to ~209 MMT in 2021/22, and the global market size was $5.50 billion in 2019 and is estimated to reach $8.48 billion by 2027.[11]

The use of heterogeneous catalysts for such processes is industrially practically set, as their homogeneous counterparts suffer from practical issues, such as recyclability, catalyst lifespan, and ease of separation, which reduce process costs and time.[1,12] The inherent characteristics of the catalyst employed for WCO conversion play a pivotal role in tuning the selectivity toward distinct product types. In the context of WCO catalytic cracking, molecular sieve catalysts, such as H-ZSM-5, metal-impregnated MCM-41 and Y-zeolites demonstrated in many aspects good performance associated to their specific

[a] Dr. I. F. Silva, I. Shekova, A. Volkel, Prof. Dr. M. Antonietti
Department of Colloid Chemistry
Max Planck Institute of Colloids and Interfaces
Am Mühlenberg 1, 14476 Potsdam, Germany
E-mail: Ingrid.Silva@mpikg.mpg.de
Markus.Antonietti@mpikg.mpg.de

[b] Dr. M. Al-Naji
BasCat – UniCat BASF JointLab
Technische Universitat Berlin
Hardenbergstraße 36, Sekr. EW K-01, 10623 Berlin, Germany

Supporting information for this article is available on the WWW under https://doi.org/10.1002/cssc.202301786

features, including a large surface area, high thermal stability and tailorable pore size.[7,13] However, the resulting pyrolysis oils from these studies exhibited high acid values, which can be a threat to car engines due to corrosive characteristics, and substantial viscosity, preventing their utilization in internal combustion engines.[13] In addition, silica-based catalysts are inherently sensitive to water at the applied elevated temperatures, which restricts the spectrum of "waste" to be converted.[14]

Carbocatalysis has emerged as a prominent strategy to tackle questions of water sensitivity or tolerance against polar impurities.[15–18] This approach involves the incorporation of acidic sites into carbon nanomaterials, giving rise to acid catalysts that improve the biofuel quality through more selective catalytic reactions, addressing the issues of extreme corrosiveness and viscosity.[16] As a source of acid catalysts, Na-lignosulfonate (LS), a by-product of paper manufacturing, was used for the first time by Konwar and Mikkola to build up a highly porous material with sulfonate groups and carbonaceous resins used for acetalization of glycerol to solketal production.[19] The aforementioned work paved the way for a large number of LS catalytic applications. For example, such acidic resins were later applied by the same group for the heterogeneous catalysis of transesterification reactions toward high-value monoglycerides and carbon-carbon coupling of biobased furans to branched C_{16}–C_{18} petrochemicals.[20,21] In addition, Al-Naji *et al.* described the application of LS-based acidic carbon material for the depolymerization of high-density polyethylene (HDPE) and a real blend of low-density and high-density polyethylene (LDPE and HDPE) plastic waste to produce hydrocarbons.[18] Eren *et al.* used LS to synthesize a sulfur-doped carbon anode material coated with carbon nitride thin films by CVD to exploit the electrochemical activity of this material.[22] Hong *et al.* showed the use of a one-pot cascade method to produce 2,5-diformylfuran directly from glucose through a carbocatalyst synthesized from $Al(NO_3)_3$ supported on porous carbon derived from LS or a mixture of LS and Na-polystyrene.[23]

Herein, the design of a versatile and inexpensive LS-based hierarchical acidic carbocatalyst (CZnLS950) is applied to produce high-quality biofuel through the pyrolysis of WCO and crude natural-oil extracted from sunflower seeds, thereby supporting the circular economy principles. LS was used as a carbon source and provided acid groups, while nano-ZnO (20 nm) templates were utilized as hard templates to create the hierarchical pores within the LS-based structure. Furthermore, to facilitate the catalyst's applicability in industrial settings, it was synthesized in pellet form, enabling easy separation from the biofuel generated during the reaction. The effects of the catalytic fragmentation reaction parameters were systematically investigated, including temperature, catalyst loading and reaction time, on WCO conversion. The recovery and reusability of the catalyst over multiple catalytic cycles and the impact on the biodiesel production efficiency were also analyzed. In addition, the gaseous phases were studied to explain the difference between conversion and liquid yield, as well as to obtain additional information on the catalytic mechanisms involved in the two oils pyrolysis.

Results and Discussion

Physicochemical Characteristics of the Synthesized Acid Carbocatalyst Pellets

The synthetic strategy for the CZnLS950 pellets is shown schematically in Figure 1. The catalyst was produced from a mechanical mixture of Na-lignosulfonate (LS), which is a by-product of paper industry, and zinc oxide (ZnO) with particle size of 20 nm. LS acts as a source of carbon and acid groups, i.e. $-SO_3H$, and ZnO as a hard template porogen.[22] A solution of urea, glucose and water was used as a binder and added into the homogeneous powder to allow the dough to be extruded from a noodle machine.[24] Then, the ZnLS was dried, manually cut into pellets (length = 7 mm and diameter = 4 mm) and carbonized at 950 °C (CZnLS950). *More details about the synthesis procedure can be found in the Experimental Section.*

The CZnLS950 catalyst was characterized by elemental analysis (EA) and the obtained results are shown in Table 1. The sulfur and oxygen contents are attributed to the products of sulfonates groups ($R–S(=O)_2-O^-$) of the LS precursor. Indeed,

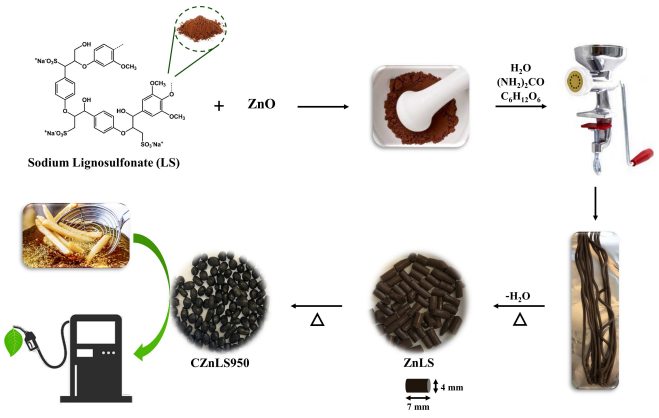

Figure 1. Schematic illustration of synthetic protocol for CZnLS950 using Na-lignosulfonate (LS) and zinc oxide (ZnO) as precursors followed by carbonization at 950 °C, as well as its application as a catalyst for biofuel production from WCO.

Table 1. Summary of the CZnLS950 composition according to EA and ICP-OES; and data extracted from N_2 isotherms at 77 K.

Material	C (wt.%)[a]	H (wt.%)[a]	N (wt.%)[a]	S (wt.%)[a]	O (wt.%)[a]	Zn (wt.%)[b]	Na (wt.%)[b]	S_{BET} (m^2/g)[c]	P_d (nm)[d]
CZnLS950	65.4 (±1.0)	1.5 (±0.4)	1.6 (±0.1)	9.7 (±0.3)	12.8 (±0.4)	2.8 (±0.8)	2.6 (±0.4)	280.0	3.83

[a] C, H, N and S contents from EA; [b] Metals percentage from ICP-OES analysis; [c] Specific surface area calculated using Brunauer-Emmett-Teller (BET) equation; [d] pore size distribution (P_d) calculated by Barrett-Joyner-Halenda (BJH) method.

coal desulfurization occurs from 600 °C, but the presence of the S-containing groups in the material synthesized at 950 °C indicates a significant physical and chemical stabilization.[16,25] Usually these groups appear in the catalyst as edge terminations, as previously discussed by Al-Naji *et al.*, and the "nobility" of the catalyst resulting from a changed collective electron density and insertion of active sites was described.[16,18] In addition, during the carbonization process of CZnLS950 synthesis, gaseous products (H_2O and CO_x) are released, which reduce the O content by about 12 wt.% in relation to the S content, i.e. the acid sites are not necessarily sulfonic acids. Interestingly, zinc and sodium contents were noticed in small quantities in the catalyst by inductively coupled plasma-optical emission spectrometry (ICP-OES) analysis. The majority of zinc is removed by evaporation at temperatures above 907 °C, while the residuals were attempted to be removed by washing out with HCl after thermal condensation (see experimental section).[22,26]

The thermogravimetric (TG) and derivative TG (DTG) curves obtained in synthetic air and N_2 atmospheres showed good thermal stability up to 450 °C and 800 °C, respectively (Figures 2a and S1a). Notably, both curves exhibited a small weight loss around 350 °C, indicative of catalyst operational stability close to this temperature and attributed to the removal of sulfone-like groups, similar to classical sulfur-carbon materials described in the literature.[27,28] A small weight loss of ~6 wt.% around 100 °C, in the curve obtained using synthetic air, can be assigned to the loss of surface adsorbed moisture present in the material. The residue observed of ~14 wt.% is mainly attributed to ash content, based on the remaining zinc and sodium (Figure 2a).[18] The surface area analysis of the catalyst was investigated by N_2 adsorption/desorption isothermal curves and calculated using the Brunauer-Emmett-Teller (BET) method (Figure 2b and Table 1). The BET surface area of CZnLS950 catalyst was 280 $m^2 g^{-1}$. The corresponding pore size distribution measurement was evaluated using desorption data with the Barrett-Joyner-Halenda (BJH) method and revealed predominantly mesoporous structures characterized by sizes ranging from 3–5 nm (Figure 2b-insert and Table 1), i.e. these pores are big enough for oil molecules to enter. For a perspective analysis, BET surface area and corresponding pore size distribution calculations were also conducted for the pristine ZnLS material and the values obtained were 1.1 $m^2 g^{-1}$ and 0.53 nm, respectively, as illustrated in Figure S2 and detailed in Table S1. The distinctive hierarchical mesoporosity exhibited by CZnLS950 is primarily attributed to the utilization of ZnO as a structural template, allowing the access of oil to a larger number of active sites.[29,30] According to the IUPAC classification, the shape of the isotherm for CZnLS950 belongs to type IV, characteristic of mesoporous materials with multilayer adsorption followed by capillary condensation of nitrogen in the mesopores.[31,32]

Scanning electron microscopy (SEM) was used to observe the morphology of the CZnLS950 (Figure 3a–b). The images indicate the existence of a smooth surface with dense coating and hierarchical porous networks, inherited from the ZnO nanostructures template, which structurally explains the N_2 adsorption-desorption isotherm.[30] The powder XRD diffractogram of CZnLS950 material presents two broad peaks at 23° and 43° corresponding to the (002) and (100) diffraction planes of graphitic carbon, respectively, indicating weakly ordered carbons (Figure S1c).[22,32] Yu *et al.* demonstrated that increasing of pyrolysis temperature of the nano-ZnO/gelatin composites improved the graphitization degree of the material, confirmed by the sharpest peak at 43° obtained for the material treated at 950 °C.[32] Ruz *et al.* established a similar correlation in their study focusing on material synthesized from sucrose and zeolite. In this case, increasing the annealing temperature from 700 °C to 900 °C leads to more prominent peaks within the XRD patterns, closely linked to the enhanced carbon order.[33] The same effect was observed for the material synthesized in this work, evidenced by the accentuation of the peak at 43°. In addition, high-resolution transmission electron microscopy (HRTEM) images obtained for CZnLS950 confirm the presence of a highly porous structure with thin and rather extensive bent carbon walls (Figure 3c–d). A higher degree of graphitization, even with bend layers, was described to be beneficial for a number of catalytic applications.[32,34] TEM measurement with

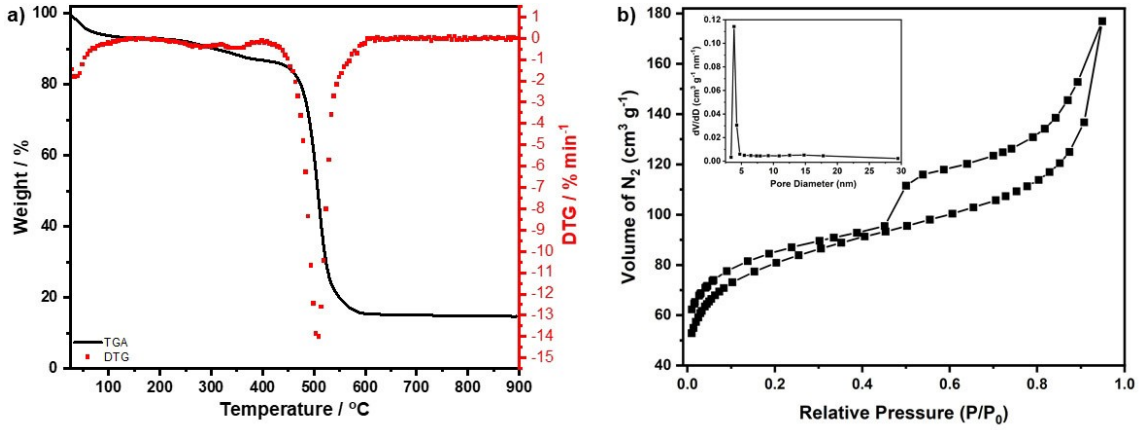

Figure 2. a) TG and DTG curves performed in dynamic synthetic air atmosphere (50 mL min^{-1}) in alumina crucible with heating ratio of 10 °C min^{-1} and b) Nitrogen adsorption-desorption isotherm for CZnLS950 material. Inlet in (b) pore size distribution by BJH method for CZnLS950 material.

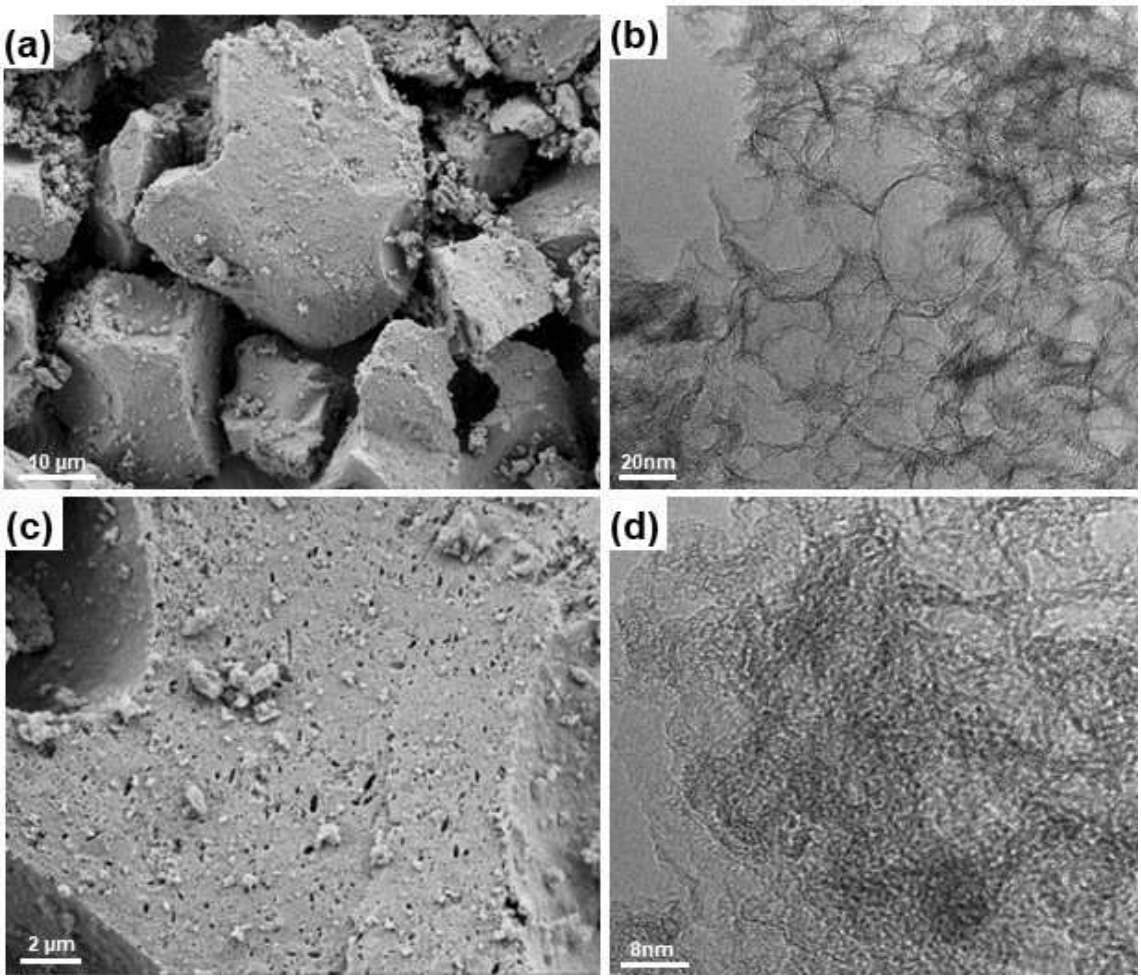

Figure 3. a–b) SEM images and c–d) HRTEM images of CZnLS950 material.

electron dispersive X-Ray mapping (TEM-EDX) revealed a homogeneous distribution of the elements: C, O, Na, S and Zn throughout the catalyst structure (Figure S3). Raman spectrum of CZnLS950 is presented in Figure S4b and showed two broad bands, in which a strong band at 1350 cm^{-1} (D-band) is related to the lattice defect of carbon atoms and a weak band at 1580 cm^{-1} is associated to the in-plane stretching vibration modes of sp^2 hybridized carbon atoms in a 2D hexagonal lattice of typical graphite.[35,36] The relative intensities of these two bands indicate that the carbon structure in CZnLS950 is composed of heteroatom- and structure-wise rather disordered, in agreement with the other characterizations. Furthermore, the FTIR of the ZnLS material showed bands characteristic of Na-LS and, which are absent in CZnLS950 (Figure S4a).

The density of acid sites (DAS) was quantified by temperature-programmed desorption (TPD) of ammonia, NH_3-TPD (Figure S1b). The analysis unveiled three different NH_3 desorption peaks at 188 °C (low-temperature region peak), 402 °C (medium-temperature region peak) and 663 °C (high-temperature region peak). These peaks correspond to differing strengths of acid sites: weak, medium, and strong, respectively. The cumulative DAS was 1100 µmol NH_3 g^{-1} (1.1 mmol g^{-1}), in alignment with values reported in previous studies of analogous materials.[18] Majd *et al.* analyzed a similar material to the one reported herein by X-ray photoelectron spectroscopy (XPS) analysis and attributed the medium-strong binding of NH_3 to the presence of sulfone-like groups. These species bear a resemblance to electron-poor sulfones embedded within the conjugated backbone of the carbon catalyst, which exhibits thermal stability and a comparable high alpha-C acidity. Moreover, the authors also found different carbon edge terminations with acidity, i.e., –COOH and phenolic C–OH, which explain the low and medium temperature peaks in the NH_3-TPD profile.

The characterization of CZnLS950 across several techniques led to the conclusion that it contains sulfone-like groups in a conjugated carbon framework, which enables it to act as a catalyst with acidic characteristics. Additionally, its hierarchical mesoporous structure provides a high surface area for the reactants to interact with the catalyst's active sites. Overall, the characterizations of CZnLS950 demonstrate its potential as an effective and inexpensive solution, synthesized from a paper-making by-product, for use in mild-temperature acid catalysis.

Thermal and Catalytic Pyrolysis of WCO

To evaluate how the properties of CZnLS950 affect its catalytic efficiency, the material was tested for WCO catalyzed thermal fragmentation. It is widely recognized that non-catalytic thermal pyrolysis often yields low-quality oil containing oxygenated compounds (ketones, aldehydes, carboxylic acids, alcohols and phenols).[37] The introduction of CZnLS950 in the thermal decomposition can enhance the quality of the resulting bio-oil by facilitating additional reaction processes such as dehydration, decarboxylation, and decarbonylation. The pyrolysis and catalytic pyrolysis experiments were carried out in a laboratory-scale batch reactor (*see experimental section for more details*).

WCO composition in the side chains is 82 wt.% of palmitic acid (C_{16}) and 15 wt.% of oleic acid (C_{18}), with the remaining 3 wt.% being some other fatty acids (FAs) (Table S2). Awogbemi *et al.* conducted a comparative analysis of the FAs composition in WCO obtained from different forms. Their study highlighted the composition of WCO from the French fries process spanning from 15 to 73 wt.% saturated fatty acids (SFAs), 6 to 27 wt.% monounsaturated fatty acids (MUFAs) and 0 to 79 wt.% polyunsaturated fatty acids (PUFAs).[38] Overall, the FAs composition of WCO inherently hinges upon the specific food type employed for frying. In the case of the WCO used in this work, which also comes from the French fries process, the oil composition is 82 wt.% of SFAs, 15 wt.% of MUFAs and 3 wt.% of PUFAs. Indeed, the repeated exposure of WCO to high-temperature cooking processes can contribute to elevated SFAs levels.

The thermal decomposition of WCO was tested at a comparably mild temperature, i.e. 340 °C. This temperature is just above the thermodynamic stability point of alkanes, since not even catalysis can act against thermodynamics. Higher temperatures would be faster, but the present data set intends to analyze intermediates and potentially poor conversion pathways in follow-up reactions. The results revealed that the thermal cracking of WCO (Table 2 - entries 2 and 6) indeed occurred even without any catalyst. Catalytic pyrolysis using CZnLS950 was also assessed under the same conditions, and a higher product yield in the gaseous phase was observed in relation to the non-catalytic process (Table 2 - entries 3 and 7), indicating the presence of multiple cracking events already at 340 °C, in other words the catalyst promotes the cracking of WCO into lighter hydrocarbons. Although no significant differences were noted in the liquid and gaseous yields between reactions with and without catalyst, the quality of the oil produced without catalyst is notably lower. The crude oil obtained without the catalyst contains a significant amount of acids (~9 wt.%) and ketones (~34 wt.%), in good agreement with previous data on the thermolysis of fats, also resulting in the described performance loss for combustion purposes (Figure 4a).[39] High acidity values and high oxygen contents are always found in the bare thermal process, which is directly associated with unacceptable biofuel quality.[39]

In addition, to better understand the structure-activity relationship of the catalyst, the WCO pyrolysis was performed with the starting reagents used in the CZnLS950 synthesis and with the catalyst before the carbonization process to observe the influence of these materials on the reaction and to elucidate the real role of CZnLS950. As illustrated in Figure 4a, the pyrolysis reaction with LS exhibited an even higher number of acid groups (~17 wt.%) at the end of the reaction. A parallel investigation was conducted with an equivalent percentage of Zn in CZnLS950 catalyst. ZnO was employed and the results showcased a notably reduced generation of acid groups (~2 wt.%) compared to the non-catalytic reaction, indicating that Zn plays an important role in the reaction. However, the reaction with ZnO showed a pronounced abundance of ketone groups. The mechanical mixture of LS and ZnO, ZnLS, synthesized prior to the carbonization process, was also tested and revealed the absence of acid groups in the produced biofuel (Figure 4a). Nevertheless, ~28 wt.% of ketones were observed, of which 70 wt.% correspond to 16-Hentriacontanone, indicating the occurrence of ketonization of carboxylic acids through decarboxylation, a process involving the conversion of two carboxylic acids into a carbonyl group, carbon dioxide and water.[40,41] From an ecological perspective, this process stands out for its cleanliness without the need for solvents or another elaborate reagent. Furthermore, roughly 44 wt.% of the hydrocarbons formed were C15, all of them

Table 2. Reaction parameters varied in order to determine optimal conditions for the WCO pyrolysis.

Entry	Catalyst	Catalyst:WCO Ratio	Temperature/°C	Time / h	Liquid/wt.%[a]	Oil inside of the catalyst/wt.%[b]	Gas/wt.%[c]
1	CZnLS950	1:10	300	4	58	25	17
2	No catalyst	Not applicable	340	4	78	–	22
3	CZnLS950	1:10	340	4	56	10	34
4	CZnLS950	1:20	340	4	73	11	16
5	CZnLS950	1:20	340	20	66	9	25
6	No catalyst	Not applicable	340	20	81	–	19
7	CZnLS950	1:30	340	20	71	8	21
8	CZnLS950	1:50	340	20	79	7	14

[a] The yield of liquid biofuels was calculated according to Eq.1. [b] The oil remaining manually inseparable from the catalyst after reaction was calculated according to Eq.2. [c] The gas yield was estimated by mass balance. It is important to highlight that no significant amount of coke deposition was observed within the reactor at the end of the reactions.

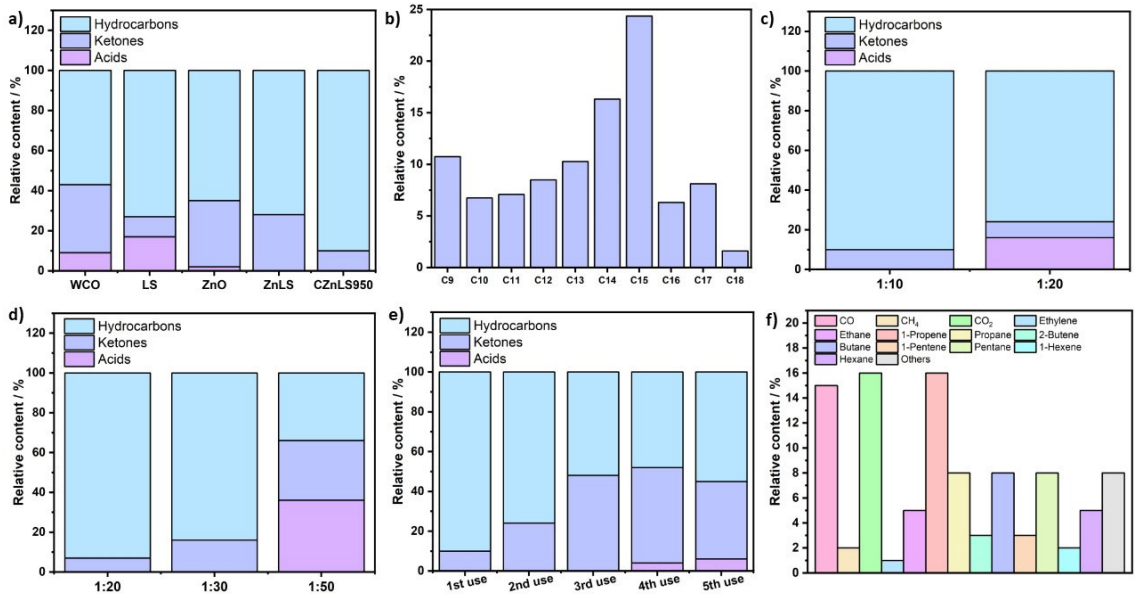

Figure 4. a) Comparison between the produced biofuel contents from the reaction of pure WCO, 1 g of LS, 0.035 g of ZnO (equivalent percentage of Zn in CZnLS950), 1 g of ZnLS and 1 g of CZnLS950. Reaction conditions: 340 °C, 10 g of WCO, 4 h. b) Relative contents of hydrocarbons produced in the condensable liquid phase. (Reaction conditions: 340 °C, 1 g of CZnLS950 : 10 g of WCO, 4 h). Optimization of the amount of WCO using CZnLS950 catalyst c) Reaction conditions: 340 °C, 1 g of CZnLS950, 4 h and d) Reaction conditions: 340 °C, 1 g of CZnLS950, 20 h. e) Recycling reactions of CZnLS950 catalyst (Reaction conditions: 340 °C, 1 g of CZnLS950 : 10 g of WCO, 4 h). f) Relative contents in the non-condensable gas produced (Reaction conditions: 340 °C, 1 g of CZnLS950 : 10 g of WCO, 4 h).

within the C9–C17 range. However, ZnLS pellets exhibited instability at the end of the reaction, resulting in significant leaching into the oil produced. Indeed, the oil obtained from the reaction using ZnLS displayed low density aggregate structures formed by flocculation. These results showed that while the ZnLS catalyst effectively removes acid groups from WCO, potentially due to the high Zn content acting as a Lewis acid site, it yields a substantial number of ketones, which in practice can pose challenges for automotive applications. On the other hand, the reaction with CZnLS950 unfolded the absence of acid groups and 90 wt.% of hydrocarbons, mainly pentadecane (~24 wt.% – Figure 4b), and 10 wt.% of oxygenated contents from ketone groups, whose main product observed was 2-heptadecanone (~32 wt.%) (Figure S5a). Overall, CZnLS950 showed a significant improvement in the quality of the biofuel produced from the catalytic pyrolysis of WCO, promoting the formation of hydrocarbons while reducing the formation of oxygen-containing compounds. This improvement can be attributed to the synergistic effect of the sulfone-like groups and a small quantity of Zn incorporated into the catalyst structure after the carbonization process.

In order to optimize the reaction conditions, several parameters were investigated, including temperature, catalyst to WCO ratio and reaction time. Temperature plays a significant role in driving the reaction rate for any catalytic reaction.[42–44] To evaluate the temperature effect, WCO catalytic pyrolysis was performed at 300 °C and 340 °C (Table 2 - entries 1 and 3). It was observed that the product obtained from the reaction performed at 300 °C is composed of 93 wt.% of acid groups and only 7 wt.% of hydrocarbons (Figure S5b). Conversely, the reaction at 340 °C showed a produced oil with 90 wt.% of hydrocarbon contents, culminating in 56 wt.% of liquid biofuel yield. Therefore, the temperature of 340 °C was chosen based on this optimized parameter.

The use of heterogeneous catalysts has big advantages in WCO pyrolysis reactions, although higher catalyst loadings are required, typically ranging from 3–15 wt.% compared to the amount of homogeneous catalyst reported to be 1 wt.% of used precursor oil.[1] While higher catalyst loadings are required in fluidized bed reactors or flow reactors, the use of pellets can facilitate separation on an industrial scale. In order to elucidate the catalyst influence, the temperature was kept at 340 °C, and the catalyst to WCO ratio was increased to 1 : 20 (Table 2 – entry 4). The produced biofuel liquid yield increased from 56 wt.% to 73 wt.%, however analyzing the produced oil, the reaction conducted with 1 : 20 ratio of catalyst to WCO yields 16 wt.% of acid groups and 8 wt.% of ketone groups (Figure 4c). To improve the biofuel quality with a higher ratio, the reaction time was elevated to 20 h (Table 2 – entries 5–8). Here, when the ratio of catalyst to WCO was increased, the yield of produced biofuel also became higher. Nevertheless, from the point of view of the quality of produced oil, the reaction exhibits good results, under these conditions, up to a ratio of 1 : 30 of catalyst to WCO, since the ratio of 1 : 50 presents 36 wt.% of acid groups in the product (Figure 4d). This points to the fact that the ketones and acids are subsequently decarbonylated or decarboxylated, according to their thermodynamic instability at those temperatures.

Yu *et al.* showed that different concentrations of Zn-modified SBA-15@MgO catalyst improved the yield of liquid

biofuels. The overall results showed an increase in the catalytic efficiency with a maximum liquid biofuel yield of 71.5 wt.%, which was achieved with ~16 wt.% of Zn impregnation on SBA-15@MgO catalyst, 1:30 of catalyst to WCO ratio, 360 °C and 100 min of reaction.[45] In this work, we present a sustainable catalyst synthesized from the paper industry by-product LS, distinguished by its unique acidic characteristics with a hierarchical mesoporous structure. Our maximal biofuel productivity with a ratio up to 1:30 of catalyst to WCO was 71 wt.% of liquid biofuel yield under the optimized conditions.

Reuse experiments were also performed under the best reaction conditions to test the catalyst stability (Figure 4e). After each reaction, the pellets were manually separated and added to a new cycle without any further treatment. The good stability of CZnLS950 was observed until the third use (2nd reuse), with the product characterized by the absence of acid groups. Despite this, between the first and third uses an increase in oxygenated groups was observed and from the fourth use onwards the presence of acid groups was noted, which was around 5 wt.% for the 4th and 5th uses. Activity drop is a recurrent problem observed in several studies, and is normally related to the gradual loss of catalyst active sites during successive cycles of catalytic cracking and deposition of solid side or coke products.[45] However, in those cases the catalyst activity is recovered by post-thermal coke burn-off or washing treatments. Therefore, catalyst reactivation with heat treatment (without additional washing) was also carried out at 350 °C for 4 h. After the second use, a relative composition of 35 wt.% of acid groups, 30 wt.% of ketone groups and 35 wt.% of hydrocarbons appeared, indicating the deterioration of active sites.

The gas phase produced during the reaction under the optimized parameters was collected at the end of the reaction at room temperature and analyzed to add additional information to understand the reaction process involved in the biofuel production from WCO (Figure 4f). It was observed that the main gases produced were CO_2 (16 wt.% from acid decarboxylation), 1-propene (16 wt.%), and CO (15 wt.% from decarbonylation). CO and CO_2 production are the key parameters to identify the different deoxygenation pathways and are mandatorily existent to remove oxygen from triglyceride molecules, which is a substantial factor for the production of high-quality biofuels with lower acidity values and higher heating values. Interestingly, unlike the rest of the trend, the 1-propene was the only alkene formed in higher proportion than its correspondent alkane, which is presumably produced from the glycerol backbone. Propylene is a value product primarily used to produce polypropylene and is an essential building block for various petrochemical manufacturing processes.[46,47] Usually for WCO pyrolysis the most commonly produced gases are CO_2 and CO, which gives this catalyst an additional role in the propylene production from a waste source. The above results indicate that the CZnLS950 promotes chemical reactions during WCO cracking, including decarbonylation, decarboxylation, hydrogenation and dehydrogenation, due to alkene formation in the gaseous and liquid phases.

The liquid biofuel analyses revealed a distribution primarily composed of hydrocarbons ranging from C9 and C17, which is similar to the composition of a typical diesel fuel (Figure 4b). The higher content of C15 can be attributed to the decarboxylation of dominant palmitic acid constituting the WCO (Table S2). Furthermore, the FTIR analysis of the biofuel demonstrated the absence of νC=O and νC–O at 1739 and 1169 cm^{-1}, respectively, characteristics of carboxylic acid groups (Figure 5a). This finding is consistent with the gas chromatography-mass spectrometry (GC-MS) results, which indicated the absence of carboxylic acid compounds in the produced biofuel. However, νC=O at 1715 cm^{-1}, attributed to the presence of ketone groups, was still observed in minor proportions in the biofuel. TGA analyses showed that the main evaporation of the produced biofuel occurs up to 200 °C. On the other hand, WCO, with its substantial number of acid groups in its structure, starts to thermally decompose at 250 °C and completes the process at 570 °C (Figure 5b). The EA analyses of the biofuel produced revealed that it consists of C (83.8 wt.%), H (12.6 wt.%) and O (3.1 wt.%) (Table S3). No sulfur or zinc was detected in the biofuel (< 0.2 wt.%). Additionally, viscosity, density and heating

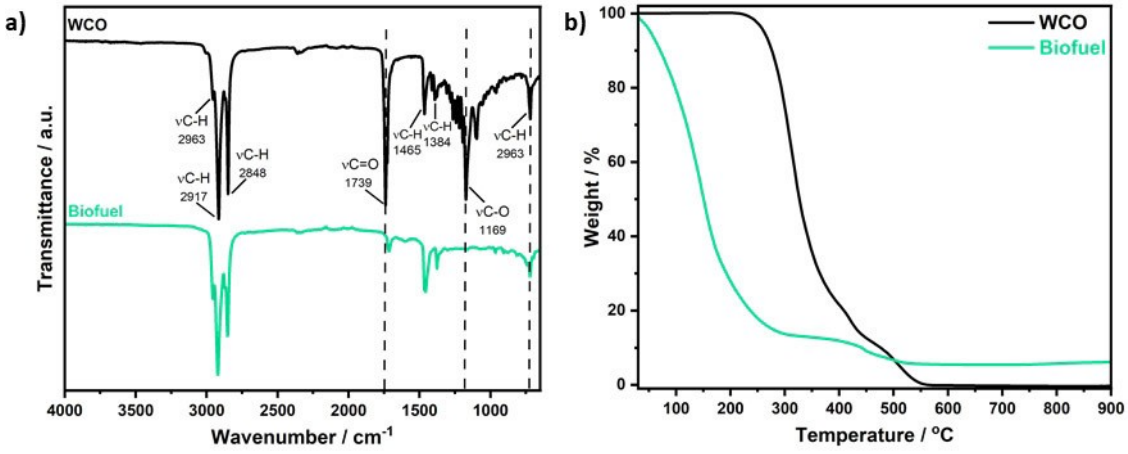

Figure 5. Comparison between the biofuel produced and the initial WCO by a) FTIR and b) TGA analyses performed in dynamic synthetic air atmosphere (50 mL min^{-1}) in alumina crucible with heating ratio of 10 °C min^{-1}.

value parameters were evaluated, resulting in values of 6.84 mPa.s at 25 °C, 0.84 g cm^{-3} and 43.9 MJ Kg^{-1}, respectively, which were compared to those of ideal diesel fuel (Table S3). The viscosity of ideal diesel fuel is 8.51 mPa.s at 25 °C, the density is 0.84 g cm^{-3} and the heating value is in the range of 42–46 MJ Kg^{-1}.[48] This indicates that the biofuel produced here, using waste oil as a resource, has significant potential to replace or blend with diesel fuel, offering a more sustainable process that can help meet future energy demands.

Kraiem *et al.* also performed WCO pyrolysis process under a nitrogen (N_2) atmosphere with a heating rate of 5 °C min^{-1} from the ambient temperature to 500 °C. A yield of ~64 wt.% of bio-oil production was obtained. Through the chemical characterization using GC/MS and FTIR, the synthesized bio-oil is a complex mixture of hydrocarbons ranging from C3 to C24 and oxygenated compounds, such as carboxylic acids, ketones, aldehydes, and alcohols.[49] In another study, Hassen Trabelsi *et al.* evaluated the effects of final temperature and heating rates of the WCO pyrolysis process using a laboratory-scale fixed-bed reactor. The authors unveiled a maximum bio-oil yield of 80 wt.% at 800 °C and 15 °C min^{-1}. The oil obtained contains a wide variety of hydrocarbons (C6 to C27), ketones and aldehydes.[50] In juxtaposition to the aforementioned studies, the present investigation distinguishes itself and shows additional findings in the sense of WCO catalytic pyrolysis under mild conditions, i.e. 340 °C, featuring pronounced biofuel production capacity, yielding 71 wt.% of liquid biofuel with relative hydrocarbon contents spanning C9 to C18, while the gaseous phase content (except carbon oxide and carbon monoxide eliminations) ranging from C2–C6. It is important to highlight the absence of acid groups in the final liquid biofuel produced, verified by GC-MS and FTIR, which indicates that the entire acid content within WCO undergoes catalytic elimination during the reaction.

To assess the catalyst's performance with alternative oil feedstocks, CZnLS950 was tested for the pyrolysis of crude natural-oil extracted from sunflower seeds, chosen as an initial example, due to Europe's significant contribution of approximately 75.8% to the global sunflower oil production.[51] Crude natural-oil from sunflower seeds typically contains longer FAs chains compared to WCO (Table S2). Therefore, pyrolysis reactions were carried out for 8 h and 24 h, using an oil to catalyst ratio of 10:1, respectively, at 340 °C (Figure S6a). After 8 hours of reaction, a substantial amount of 26 wt.% of acid groups was still observed in the produced biofuel. However, extending the reaction time to 24 h resulted in the complete absence of acid groups in the reaction product and the presence of 26 wt.% of other functional groups, i.e., ketones, aldehydes and alcohols. Analyzing the composition of the liquid biofuel, it was found that among the 76 wt.% of hydrocarbons formed, 54 wt.% corresponded to carbon chains ranging from C13 to C16 (Figure S6b). Additionally, among the 26 wt.% of the oxygenated products formed, 77 wt.% were associated with [1,1'-Bicyclohexyl]-2-one, 1'-hydroxy, which is formed through the self-condensation of cyclohexanone using a strong acidic or basic catalyst and can be used in the synthesis of pharmaceuticals and fine chemicals (Figure S6c).[52] The main gases produced were saturated hydrocarbons with chain lengths (except carbon oxide and carbon monoxide eliminations) ranging from C2 to C6 (Figure S6d). The experiments evaluated with crude natural-oil from sunflower seeds further confirmed the excellent potential of the CZnLS950 catalyst for biofuel production and the generation of value-added products also from this particular feedstock.

Mechanisms Investigation

Multiple organic reactions typically occur simultaneously during the high temperature cracking process, some catalyzed, some only thermal.[53] At high temperatures, triglyceride pyrolysis primarily yields acids, acrolein, and ketenes as the main products (step i – Figure 6).[7,53] In our investigation, two distinct pyrolysis mechanisms can be proposed using CZnLS950, based on the liquid and gaseous products obtained from the catalytic pyrolysis of WCO and crude natural-plant oil extracted from sunflower seeds (Figure 6 and Tables S4 and S5). WCO consists mainly of palmitic acid (~82 wt.% of SFAs), and the key catalytic reactions are ii) decarboxylation followed by iii) hydrogen radical transfer from the catalyst, leading to the formation of pentadecane (~24 wt.%), which is the main product of the produced hydrocarbon mixtures (Figure 6a). Another significant aspect of this reaction involves iv) ketene formation and consecutive decarbonylation, resulting in the production of alkanes and ketones (from dimerization). The fatty acids, presumably in their still activated pentadecane radical form, also undergo processes such as isomerization and fragmentation in step v, giving rise to the formation of smaller alkanes and alkenes. The light alkanes and alkenes sought in the gas phase are probably also formed in step v. Alkenes can further engage in cyclization reactions, one of the possible routes to cyclic hydrocarbon formation (step vi). These cyclic structures stay hydrogenated (~4 wt.%) or undergo catalytic dehydrogenation (~2 wt.%) (step vii), which reconstitutes the hydrogen on the surface of the carbocatalyst needed for step iii. Based on the quantitative analysis of the liquid and gaseous phases produced in these reactions, it is evident that steps ii, iii, iv, and v play pivotal roles in the pyrolysis of WCO when CZnLS950 is used as a catalyst.

On the other hand, crude natural-oil extracted from sunflower seeds is mainly composed of linoleic acid (~52 wt.% PUFAs) and oleic acid (~40 wt.% MUFAs). The longer carbon chains and especially the presence of carbon-carbon double bonds in this oil give rise to a reaction cascade distinct from the one proposed for WCO. Furthermore, the presence of double bonds in the chain interferes with the as formed radicals from decarboxylation, and hydrogen transfer, fragmentation, and dehydrogenation reactions are then favored in this cascade. Thus, the primary and the most important pathway for the pyrolysis of sunflower seeds crude natural-oil might be the cracking and isomerization of linoleic acid and oleic acid (step ii – Figure 6b), resulting in the predominant formation of alkanes, alkenes and smaller chain acids. The products from step ii are subjected to successive cracking and isomerization (step iii).

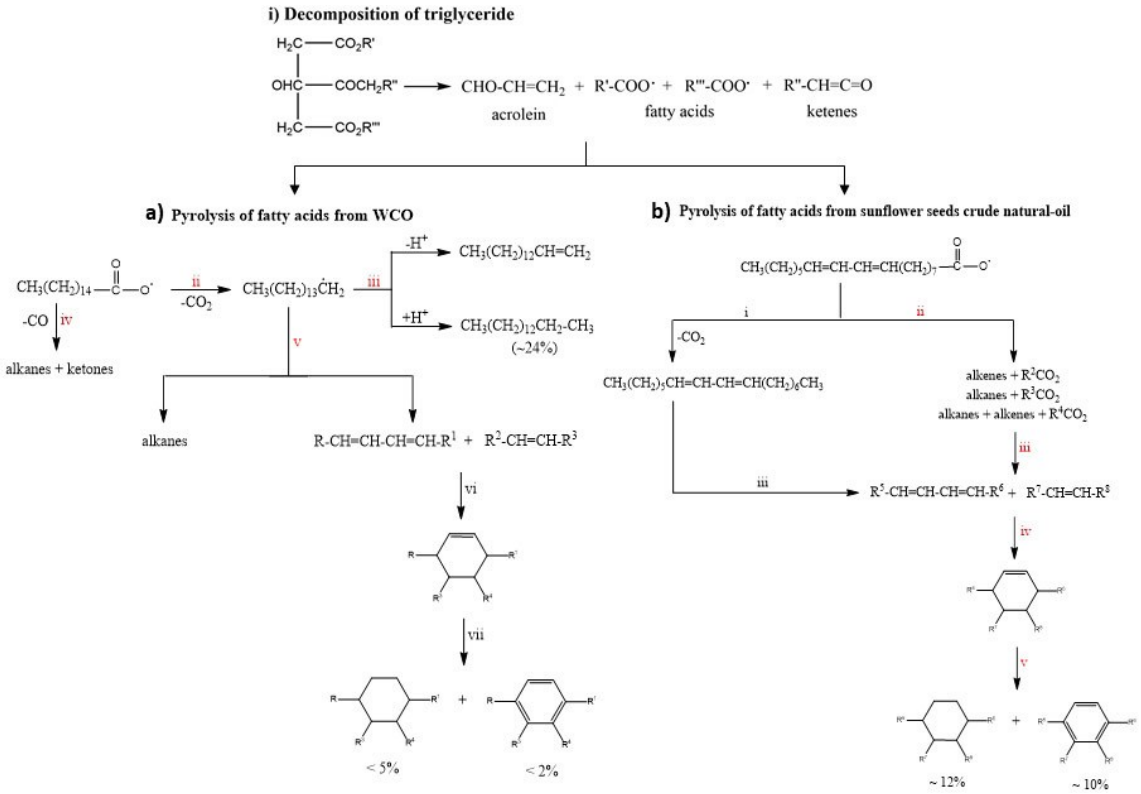

Figure 6. Proposed catalytic mechanisms for biofuels produced from the pyrolysis reactions of a) WCO and b) sunflower seeds crude natural-oil using CZnLS950 as a catalyst.

The products from step iii undergo cyclization at the alpha positions of the double bonds (step iv), and subsequently experience dehydrogenation (step v). In this secondary cascade, steps ii, iii, iv, and v appear to be faster, as evidenced by the presence of approximately 12 wt.% cycles and 10 wt.% aromatics in the product at the end of the reaction.

These insights into the pyrolysis mechanisms from both oils provide a valuable understanding of the intrinsic reactions taking place during the catalytic conversion processes, all based on the products identified by GC (Tables S4 and S5). Yu *et al.* elucidated a synergistic acid-base catalysis mechanism for biofuel synthesis using a Zn-modified SBA-15@MgO catalyst. According to their proposed mechanism, the initial step involves the adsorption of triglycerides onto zinc species featuring Lewis acid sites. Subsequently, the C–C bonds undergo cleavage, leading to the formation of short-chain fatty acids, hydrocarbons, and gas. Following this, these fatty acids are adsorbed onto magnesium oxide, which contains basic sites, resulting in the creation of a metal salt. This metal salt is then said to be further decomposed at high temperatures through deoxygenation, generating additional hydrocarbons and gas.[45] In another work, Fu *et al.* conducted studies on hydrothermal decarboxylation reactions of palmitic and oleic acids using two different activated carbons in near and supercritical water. The absence of unsaturation in the primary products was attributed to hydrogenation, with hydrogen originating from water molecules and other fatty acids. Furthermore, the presence of double bond in oleic acid was found to facilitate oligomerization pathways, resulting in the production of higher molecular weight molecules that do not elute from the GC.[54] In the context of this work, the acidic catalytic sites of the synthesized CZnLS950 material are attributed to the presence of sulfone-type groups within a conjugated carbon structure, alongside a minor zinc content (2.8 wt.%). The mesoporous structure plays a pivotal role by providing high surface area for the reactants to interact with the active sites of the catalyst. As a result, decarboxylation, decarbonylation, cracking, isomerization, hydrogenation, and dehydrogenation are identified as the key reactions within these mechanisms, with their importance varying depending on the starting oil. Furthermore, it is important to note that the possible oligomerization of acids present in sunflower oil pointed out above cannot be confirmed either due to their lack of elution in the GC.

Conclusions

The catalytic efficiency of CZnLS950 was systematically investigated for the pyrolysis reactions of WCO and crude natural-oil derived from the sunflower seed to produce biofuel fragmentation products. Multiple reaction parameters were evaluated to determine the optimum conditions, while using the minimum catalyst loading and energy consumption, to obtain the highest biofuel yield. WCO pyrolysis using CZnLS950 as the catalyst, under the optimized conditions, exhibited excellent performance in biofuel production, with a 71 wt.% of liquid oil yield

and ~3 wt.% of catalyst loading. This outcome is explained by the catalyst's distinctive acidic characteristics, resulting from the presence of sulfone-like groups, with a hierarchical mesoporous structure, which provides a high surface area for the reactants to interact with the catalyst's active sites. Moreover, the absence of acid groups in the liquid biofuel produced indicates that the entire acid content within WCO undergoes catalytic decarboxylation during the reaction. The quality of the produced biofuel was also compared to the ideal diesel fuel, demonstrating its high potential to replace or blend with diesel fuel, culminating in a more sustainable process that can contribute to meeting future energy demands and supporting the circular economy. Most importantly, attempts at distinct catalytic mechanisms for WCO and sunflower seeds crude natural-oil pyrolysis were provided to understand the processes involved in obtaining the two different biofuels produced. This work paves the way for exploring the performance of CZnLS950-based materials in achieving more sustainable and efficient biofuel production from several waste-based feedstocks and under various conditions. Additionally, CZnLS950 was synthesized in pellet form, simplifying catalyst separation from the biofuel produced and facilitating large-scale production. Although, further research is needed to address the technical and economic feasibility of applying CZnLS950-based materials on an industrial scale.

Experimental Section

Preparation of LS-Based Carbon-Supported Pellets Catalysts

ZnLS and CZnLS950 were synthesized according to the previous methods reported in the literature.[18,22] The ZnLS catalyst was synthesized following the steps: 8.0 g of urea (4 wt.%, Sigma-Aldrich) and 8.0 mL of water were placed in a balloon and heated at 103 °C with continuous stirring. After the complete solubilize of urea was added 8.0 g of D-glucose anhydrous (4 wt.%, Sigma-Aldrich) in the balloon with continuous stirring and waited around 45 minutes until the solution become yellow. 96.0 g of sodium lignosulfonate (LS) (58 wt.%, Domsjö Fabriker) was mixed with 48.0 g of ZnO nanoparticles (20 nm) in a crucible until reached a homogeneous powder. Then the water solution was added dropwise to the homogeneous powder and mixed. It was added an additional 6 mL of water dropwise so the dough is not too dry but remains crumbly. The final mixture was processed using a commercial noodle manual extruding machine (Taglia Pasta, Italy) equipped with a 1 mm PTFE die (Figure 1). All the dough was extruded through the pasta machine and dried at 70 °C overnight. Then the noodle was manually cut in medium pieces pellets between 4 mm in diameter and 7 mm in length. The glucose/urea was used as a binder to avoid the random evaporation of Zn and provide crosslinking while carbonizing the formed pellets, generating an intact rigid sulfur-rich carbon.

CZnLS950 pellets catalyst was synthesized with the heating treatment of ZnLS at 950 °C under nitrogen flow using three-step program: (I) purging the oven atmosphere with nitrogen at room temperature for 1 h; (II) increasing the temperature to 120 °C with a heating rate of 3 °C min^{-1} and maintaining it for 2 h; (III) elevating the temperature to 950 °C with a heating rate of 3 °C min^{-1} and maintaining it for 2 h, then cooling it down to room temperature. During step III, carbothermal reduction of ZnO nanoparticles to Zn metal occurs, and the Zn metal leaves the framework. The pellets were washed with 500 mL of a hydrochloride acid 1 mol L^{-1} solution to remove the residual Zn in a rounded flask for twelve hours at 50 °C with continuous stirring, followed by washing them with 5 L of water until the pH was neutral. Finally, the pellets were dried in a vacuum oven for 24 hours at 70 °C.

Catalyst Characterization

Details of the characterization techniques of CZnLS950 catalyst are shown in *Supporting Information*.

Pyrolysis Reactions

WCO Pyrolysis

The bench-scale pyrolysis experiments were performed in a Parr Instrument hydrothermal reactor, series number 4560, with a maximum volume of 300 mL. The pyrolysis reactions were carried out by placing a known amount of WCO, from the French fries process, and 1 g of catalyst in a hydrothermal reactor heated to 340 °C with a heating rate of 10 °C min^{-1}. The experiments were performed in a closed vessel, and before each experiment the reactor was purged with argon to ensure that air was removed. The effect of different catalysts was performed using 1:10 of catalyst to WCO ratio, during 4 hours at 340 °C with a heating rate of 10 °C min^{-1} and stirring of 200 rpm. The effect of catalyst to WCO ratio was evaluated using 1:10 and 1:20 of CZnLS950 to WCO ratio during 4 hours at 340 °C with a heating rate of 10 °C min^{-1} and stirring of 200 rpm. Subsequently, the experiments were carried out using 1:20, 1:30 and 1:50 of CZnLS950 to WCO ratio during 20 hours at 340 °C with a heating rate of 10 °C min^{-1} and stirring of 200 rpm. Upon reaction completion, the reactor was cooled down until room temperature and the gas phase was removed through one of the reactor outlets and analyzed by GC-MS. The liquid products (L) were manually separated from the catalyst, weighed, and analyzed by gas chromatography-mass spectrometry (GC-MS) without further purification. An easy manual separation of the liquid products from the catalyst at the end of the reaction is only possible due to its synthesis in the pellet form. In addition, the mass gain of the catalyst at the end of reactions owing to the oil, which remains manually inseparable from the catalyst (Co) was also weighed. The gas yield (G) was estimated by mass balance and analyzed by GC-MS. All pyrolysis experiments were conducted at least twice and the average value was used for analyses. It is important to highlight that at the end of the reactions, no significant amount of coke deposition was observed within the reactor. The yield (wt.%) of liquid biofuels and the oil remaining manually inseparable from the catalyst after reaction (wt.%) were calculated as follows:

$$\text{Yield (liquid biofuels) } (\%) = \frac{L}{F} \times 100\,\% \quad (1)$$

$$\text{Oil manually inseparable from the catalyst } (\%) = \frac{Co - C}{F} \times 100\,\% \quad (2)$$

where F and C are the weight of WCO and catalyst, respectively, used in the reactions.

Crude Natural-Oil from Sunflower Seeds Pyrolysis

A 500 g package of Rewe Bio sunflower seeds was purchased from the Rewe supermarket located near to the Max Planck Institute. For the extraction process, the established Soxhlet method was employed, using hexane as the solvent. The round-bottomed flask was connected to the extractor and 200 mL of hexane was added. The heating plate was set to a constant temperature of 100 °C and the extraction procedure was carried out continuously for 8 hours. The flask containing the oil extract and hexane was kept in a rotary evaporator at 50 °C to remove all the hexane from the mixture. After this process, the oil was cooled down to room temperature and then weighed (Yield: 30 %).[55]

The pyrolysis reactions using crude natural-oil from sunflower seeds were performed by placing a known amount of crude oil and 1 g of catalyst in a hydrothermal reactor heated to 340 °C with a heating rate of 10 °C min^{-1}. Before each experiment, the reactor was flushed with argon to ensure that air was removed. The experiments were carried out using 1 : 10 of CZnLS950 to crude oil ratio during 8 and 24 hours at 340 °C with a heating rate of 10 °C min^{-1} and stirring of 200 rpm. After reaction completion, the reactor was cooled down and followed the same protocols described for WCO pyrolysis.

Supporting Information

The authors have detailed catalyst characterizations and additional methodologies, including liquid and gas phase analyses. summary of the produced biofuel composition according to EA, ICP-OES, viscosity, density parameters and heating value, besides the relative contents of the liquid biofuel produced from WCO and crude natural-oil from sunflower seeds, citing additional references within the Supporting Information.[56–58]

Acknowledgements

The authors gratefully acknowledge Ursula Lubahn for technical support, Bolortuya Badamdorj for the SEM and TEM measurements, Jessica Brandt for ICP-OES measurements and Max Planck Society for the financial support. I.F.S. thanks the Alexander von Humboldt Foundation for her postdoctoral fellowship. Open Access funding enabled and organized by Projekt DEAL.

Conflict of Interests

The authors declare no conflict of interest.

Data Availability Statement

The data that support the findings of this study are available in the supplementary material of this article.

Keywords: biofuel production · waste cooking oil · pyrolysis · lignosulfonate · pellets

[1] I. F. Silva, R. D. F. Rios, O. Savateev, I. F. Teixeira, *ACS Appl. Nano Mater.* **2023**, *6*, 9718–9727.
[2] "Cutting EU greenhouse gas emissions: national targets for 2030," can be found under https://www.europarl.europa.eu/news/en/headlines/society/20180208STO97442/cutting-eu-greenhouse-gas-emissions-national-targets-for-2030, accessed: 21 April 2023.
[3] "Brazil's climate change policies State of play ahead of COP27," can be found under https://www.europarl.europa.eu/RegData/etudes/BRIE/2022/738185/EPRS_BRI(2022)738185_EN.pdf, accessed: 21 April 2023.
[4] "Climate Action Tracker," can be found under https://climateactiontracker.org/countries/usa/, accessed: 21 April 2023.
[5] M. A. Bashir, S. Wu, J. Zhu, A. Krosuri, M. U. Khan, R. J. Ndeddy Aka, *Fuel Process. Technol.* **2022**, *227*, 107120.
[6] T. V. De Medeiros, A. Macina, H. A. Bicalho, R. Naccache, *Small* **2023**, *2300541*, 1–11.
[7] Y. Wang, Q. Yang, L. Ke, Y. Peng, Y. Liu, Q. Wu, X. Tian, L. Dai, R. Ruan, L. Jiang, *Fuel* **2021**, *283*, 119170.
[8] B. Maleki, H. Esmaeili, *Ceram. Int.* **2023**, *49*, 11452–11463.
[9] M. Khan, H. Farah, N. Iqbal, T. Noor, M. Z. B. Amjad, S. S. Ejaz Bukhari, *RSC Adv.* **2021**, *11*, 37575–37583.
[10] B. H. H. Goh, C. T. Chong, H. C. Ong, T. Seljak, T. Katra˘snik, V. Józsa, J.-H. Ng, B. Tian, S. Karmarkar, V. Ashokkumar, *Energy Convers. Manage.* **2022**, *251*, 114974.
[11] "Consumption of vegetable oils worldwide from 2013/14 to 2022/2023, by oil type (in million metric tons)," can be found under https://www.statista.com/statistics/263937/vegetable-oils-global-consumption/, accessed: 21 April 2023.
[12] W. Xie, J. Li, *Renewable Sustainable Energy Rev.* **2023**, *171*, 113017.
[13] G. Su, H. C. Ong, M. Mofijur, T. M. I. Mahlia, Y. S. Ok, *J. Hazard. Mater.* **2022**, *424*, 127396.
[14] M. S. Azam, C. Cai, J. M. Gibbs, E. Tyrode, D. K. Hore, *J. Am. Chem. Soc.* **2020**, *142*, 669–673.
[15] S. Navalon, A. Dhakshinamoorthy, M. Alvaro, M. Antonietti, H. García, *Chem. Soc. Rev.* **2017**, *46*, 4501–4529.
[16] M. Antonietti, N. Lopez-Salas, A. Primo, *Adv. Mater.* **2019**, *31*, 1805719.
[17] M. Al-Naji, F. Brandi, B. Kumru, M. Antonietti, *ChemCatChem* **2023**, *15*, 1–7.
[18] M. Al-Naji, M. Antonietti, *ChemSusChem* **2023**, *e202201991*, 1–7.
[19] L. J. Konwar, A. Samikannu, P. Mäki-Arvela, D. Boström, J. P. Mikkola, *Appl. Catal. B* **2018**, *220*, 314–323.
[20] L. J. Konwar, P. Mäki-Arvela, N. Kumar, J. P. Mikkola, A. K. Sarma, D. Deka, *React. Kinet. Mech. Catal.* **2016**, *119*, 121–138.
[21] L. J. Konwar, A. Samikannu, P. Mäki-Arvela, J. P. Mikkola, *Catal. Sci. Technol.* **2018**, *8*, 2449–2459.
[22] E. O. Eren, E. Senokos, Z. Song, E. B. Yılmaz, I. Shekova, B. Badamdorj, I. Lauermann, N. V. Tarakina, M. Al-Naji, M. Antonietti, P. Giusto, *J. Mater. Chem. A* **2022**, *11*, 1439–1446.
[23] M. Hong, Y. Liu, H. Sun, L. He, J. Zhu, H. Wang, S. Wang, L. Li, *Catal. Sci. Technol.* **2023**, *13*, 1335–1344.
[24] F. Brandi, M. Bäumel, V. Molinari, I. Shekova, I. Lauermann, T. Heil, M. Antonietti, M. Al-Naji, *Green Chem.* **2020**, *22*, 2755–2766.
[25] D. Liu, W. Zhou, J. Wu, *Korean J. Chem. Eng.* **2016**, *33*, 1837–1845.
[26] R. B. Gordon, T. E. Graedel, M. Bertram, K. Fuse, R. Lifset, H. Rechberger, S. Spatari, *Resour. Conserv. Recycl.* **2003**, *39*, 107–135.
[27] T. Takahashi, M. Yamagata, M. Ishikawa, *Prog. Nat. Sci. Mater. Int.* **2015**, *25*, 612–621.
[28] L. J. Konwar, P. Mäki-Arvela, E. Salminen, N. Kumar, A. J. Thakur, J. P. Mikkola, D. Deka, *Appl. Catal. B* **2015**, *176–177*, 20–35.
[29] B. Yan, J. Zheng, F. Wang, L. Zhao, Q. Zhang, W. Xu, S. He, *Mater. Des.* **2021**, *201*, 109518.
[30] M. K. Kim, D. Kim, J. Y. Seo, O. Buyukcakir, A. Coskun, *CrystEngComm* **2017**, *19*, 4147–4151.
[31] M. Thommes, K. Kaneko, A. V. Neimark, J. P. Olivier, F. Rodriguez-Reinoso, J. Rouquerol, K. S. W. Sing, *Pure Appl. Chem.* **2015**, *87*, 1051–1069.
[32] S. Yu, H. Wang, C. Hu, Q. Zhu, N. Qiao, B. Xu, *J. Mater. Chem. A* **2016**, *4*, 16341–16348.
[33] P. Ruz, S. Banerjee, M. Pandey, V. Sudarsan, P. U. Sastry, R. J. Kshirsagar, *Solid State Sci.* **2016**, *62*, 105–111.
[34] P. Strubel, S. Thieme, T. Biemelt, A. Helmer, M. Oschatz, J. Brückner, H. Althues, S. Kaskel, *Adv. Funct. Mater.* **2015**, *25*, 287–297.
[35] F. Su, C. K. Poh, J. S. Chen, G. Xu, D. Wang, Q. Li, J. Lin, X. W. Lou, *Energy Environ. Sci.* **2011**, *4*, 717–724.

[36] I. F. Silva, W. D. Do Pim, I. F. Teixeira, W. P. Barros, A. P. C. Teixeira, G. M. Do Nascimento, C. L. M. Pereira, H. O. Stumpf, *J. Phys. Chem. C* **2016**, *120*, 1245–1251.
[37] M. H. M. Ahmed, N. Batalha, H. M. D. Mahmudul, G. Perkins, M. Konarova, *Bioresour. Technol.* **2020**, *310*, 123457.
[38] O. Awogbemi, E. I. Onuh, F. L. Inambao, *Int. J. Low-Carbon Technol.* **2019**, *14*, 417–425.
[39] J. Xu, J. Jiang, J. Zhao, *Renewable Sustainable Energy Rev.* **2016**, *58*, 331–340.
[40] M. Renz, *Eur. J. Org. Chem.* **2005**, 979–988.
[41] M. Dourado, N. Fonseca, R. Fréty, E. A. Sales, *J. Braz. Chem. Soc.* **2022**, *33*, 1263–1272.
[42] V. A. Luciano, F. G. De Paula, P. S. Pinto, C. D. Prates, R. C. G. Pereira, J. D. Ardisson, M. G. Rosmaninho, A. P. C. Teixeira, *Fuel* **2022**, *310*, 122290.
[43] V. A. Luciano, D. M. Perígolo, M. G. Rosmaninho, A. P. C. Teixeira, *Fuel* **2020**, *261*, 116456.
[44] F. Brandi, M. Antonietti, M. Al-Naji, *Green Chem.* **2021**, *23*, 9894–9905.
[45] Y. Shitao, X. Cao, S. Wu, Q. Chen, L. Li, H. Li, *Ind. Crops Prod.* **2020**, *150*, 112362.
[46] J. Wang, C. Ma, J. Liu, Y. Liu, X. Xu, M. Xie, H. Wang, L. Wang, P. Guo, Z. Liu, *J. Am. Chem. Soc.* **2023**, *145*, 6853–6860.
[47] S. Qian, J. Hu, X. Wang, L. Yang, X. Suo, Z. Wang, X. Cui, H. Xing, *AIChE J.* **2023**, *69(7):e18*091.
[48] J. S. Chang, J. C. Cheng, T. R. Ling, J. M. Chern, G. Bin Wang, T. C. Chou, C. T. Kuo, *J. Taiwan Inst. Chem. Eng.* **2017**, *73*, 1–11.
[49] T. Kraiem, A. Ben Hassen, H. Belayouni, M. Jeguirim, *Environ. Sci. Pollut. Res. Int.* **2017**, *24*, 9951–9961.
[50] A. Ben Hassen Trabelsi, K. Zaafouri, W. Baghdadi, S. Naoui, A. Ouerghi, *Renewable Energy* **2018**, *126*, 888–896.
[51] V. Havrysh, A. Kalinichenko, P. Pysarenko, M. Samojlik, *Processes* **2023**, *11*, 1–14.
[52] D. Lorenzo, A. Santos, E. Simón, A. Romero, *Ind. Eng. Chem. Res.* **2013**, *52*, 2257–2265.
[53] A. Kubátová, Y. Luo, J. Šťávová, S. M. Sadrameli, T. Aulich, E. Kozliak, W. Seames, *Fuel* **2011**, *90*, 2598–2608.
[54] J. Fu, F. Shi, L. T. Thompson, X. Lu, P. E. Savage, *ACS Catal.* **2011**, *1*, 227–231.
[55] C. H. Fornasari, D. Secco, R. F. Santos, T. R. B. Da Silva, N. B. G. Lenz, L. K. Tokura, M. L. Lenz, S. N. M. De Souza, L. A. Z. Junior, F. Gurgacz, *Renewable Sustainable Energy Rev.* **2017**, *80*, 121–124.
[56] N. S. Abdelrahman, E. Galiwango, A. H. Al-Marzouqi, E. Mahmoud, *Biomass Convers. Biorefinery* **2022**, DOI 10.1007/s13399-022-02902-6.
[57] L. Klapiszewski, A. Jamrozik, B. Strzemiecka, D. Matykiewicz, A. Voelkel, T. Jesionowski, *Int. J. Mol. Sci.* **2017**, *18*, 1–19.
[58] S. S. Lam, W. A. Wan Mahari, Y. S. Ok, W. Peng, C. T. Chong, N. L. Ma, H. A. Chase, Z. Liew, S. Yusup, E. E. Kwon, D. C. W. Tsang, *Renewable Sustainable Energy Rev.* **2019**, *115*, 109359.

Manuscript received: November 30, 2023
Revised manuscript received: February 22, 2024
Accepted manuscript online: April 8, 2024
Version of record online: May 16, 2024